

Normal-incidence spectroscopic ellipsometry for critical dimension monitoring

Hsu-Ting Huang, Wei Kong, and Fred Lewis Terry, Jr.^{a)}

Department of Electrical Engineering and Computer Science, University of Michigan, Ann Arbor, Michigan 48109-2122

(Received 24 October 2000; accepted for publication 19 April 2001)

In this letter, we show that normal-incidence spectroscopic ellipsometry can be used for high-accuracy topography measurements on surface relief gratings. We present both experimental and theoretical results which show that spectroscopic ellipsometry or reflectance-difference spectroscopy at near-normal incidence coupled with vector diffraction theory for data analysis is capable of high-accuracy critical dimension (CD), feature height, and sidewall angle measurements in the extreme submicron regime. Quantitative comparisons of optical and cross-sectional scanning electron microscopy (SEM) topography measurements from a number of 350 nm line/space reactive-ion-etched Si gratings demonstrate the strong potential for *in situ* etching monitoring. This technique can be used for both *ex situ* and *in situ* applications and has the potential to replace the use of CD-SEM measurements in some applications. © 2001 American Institute of Physics. [DOI: 10.1063/1.1378807]

Critical dimension (CD) scanning electron microscopy (SEM) is the primary method used for linewidth measurement in microelectronic manufacturing.¹ However, CD SEMs are relatively slow, *ex situ*-only instruments. Optical reflection techniques employing quantitative analysis of diffraction from gratings have been explored as possible supplementary measurements to CD SEMs.^{2–4} The scattered light from gratings produces strong structures (Wood's anomalies⁵) in reflectance spectra—both as a function of angle of incidence (AOI) (Refs. 6 and 7) and wavelength^{8–10} which are very sensitive to the topography of the grating. Fixed-AOI, specular-mode spectroscopic ellipsometry (SE) or spectroscopic reflectometry (SR) measurements are highly advantageous versus angle-scanning approaches for high-speed and/or *in situ* measurements. The sensitivity of ellipsometric measurements to the topography of diffraction gratings has been reported previously,¹¹ but it has only recently been seriously explored as a metrology tool due to the development of computer modeling tools for quantitative data analysis.

In this letter, we show that while off-normal measurements ($\sim 65^\circ$ – 75°) are best for unpatterned thin-film measurements,¹² SE at near-normal incidence is strongly advantageous for topographic analysis of periodic gratings. Both our experimental and theoretical results show that SE/RDS (reflectance-difference spectroscopy) at near-normal incidence coupled with vector diffraction theory for data analysis is capable of high-accuracy CD, feature height, and sidewall angle measurements for deep submicron periodic patterns. To model the ellipsometric measurements of gratings, we have employed an accurate, full-vector simulation method—rigorous couple wave analysis (RCWA).^{13,14}

Our theoretical and experimental data will be presented from the viewpoint of SE, but it should be noted that the normal-incidence (NI) SE signals are closely related to the

reflectance-difference spectroscopy^{15,16} quantity:

$$(\Delta\tilde{r}/\tilde{r}) = 2 \frac{r_p - r_s}{r_p + r_s} = 2 \frac{\rho - 1}{\rho + 1}, \quad (1)$$

where we have assumed the sample and optical axes have been aligned and r_p and r_s are the usual complex reflectivities. In particular, for a rotating polarizer SE with a fixed analyzer at 45° , the measured intensity $I(t)$ is given by well-known equations:

$$I(t) = I_0 [1 + \alpha \cos(2\omega_p t) + \beta \sin(2\omega_p t)], \quad (2)$$

$$\alpha = \frac{\tan^2 \psi - 1}{\tan^2 \psi + 1} = \frac{|\rho|^2 - 1}{|\rho|^2 + 1} = \frac{|r_p|^2 - |r_s|^2}{|r_p|^2 + |r_s|^2}, \quad (3)$$

$$\beta = \frac{2 \cos(\Delta) \tan \psi}{\tan^2 \psi + 1} = \frac{2 \operatorname{Re}(\rho)}{|\rho|^2 + 1} = \frac{2 \operatorname{Re}(r_p r_s^*)}{|r_p|^2 + |r_s|^2}, \quad (4)$$

where all quantities have their usual meanings in the context of ellipsometry. The use of RDS at near NI to separate small surface anisotropies from bulk thin-film effects was the inspiration for this work. We should note, however, that for intentional gratings the anisotropy is much larger than that observed by RDS in epitaxial growth experiments.

There are two reasons we expect the NI technique can extract the most information on the grating profiles from SE data. First, at NI, the only mechanism causing reflectance difference of *s*- and *p*-polarized light is the grating pattern. For unpatterned structures with isotropic or uniaxial films with the extraordinary axis oriented perpendicular to the surface, there is no reflectance anisotropy ($r_p = r_s$). Thus, the SE signal is most sensitive to the presence of the grating at NI. Second, NI maximizes the illumination of the sidewalls of the grating lines (for positively sloped sidewalls), and thus has the potential for greater sensitivity to sidewall structure, particularly as the feature height increases. For off-normal techniques, shadowing effects will reduce the sensitivity of the measurement to sidewall features.

^{a)}Electronic mail: fredty@umich.edu

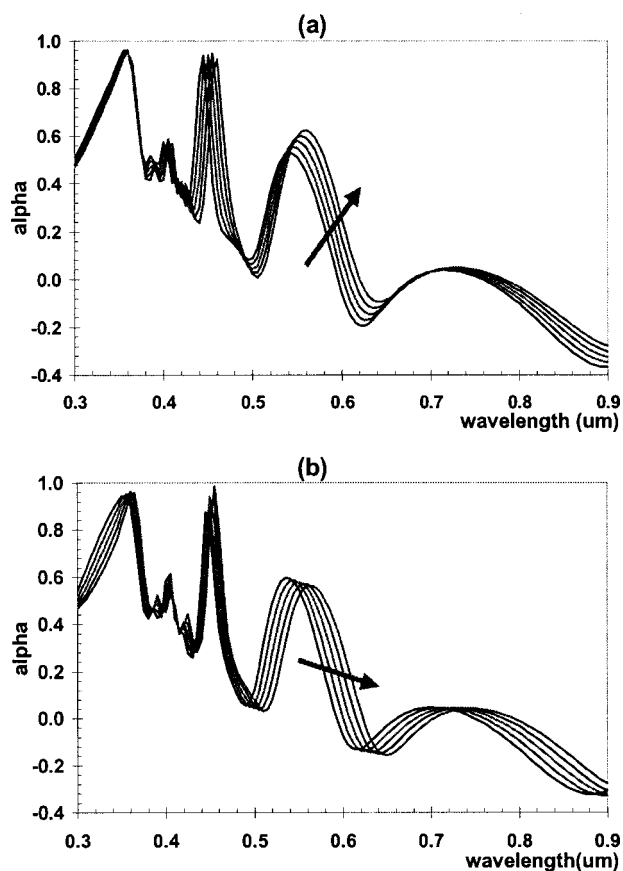


FIG. 1. At near-normal (6°) incidence SE/RDS simulation of the submicron MOSFET structure: (a) varying the CD with a step of 2% (1 nm) and (b) varying the gate height (grating depth) with a step of 2% (5 nm).

To demonstrate that NI is superior to oblique incidence for grating profile extraction, we have simulated the SE spectra for a grating test structure appropriate for deep submicron metal–oxide–semiconductor field-effect transistor (MOSFET) gates. This binary grating profile has a period of 100 nm, a CD of 50 nm, and a gate height (grating depth) of 250 nm. The ellipsometric results are represented in terms of α and β . The SE simulations at an experimentally achievable 6° AOI are shown in Fig. 1. The arrows on the plots indicate the approximate directions of movement of the major features of the spectra as the CD or depth of the gate profile is varied. Figure 1(a) shows the change of spectra when varying the CD with a step of 2% (1 nm), and Fig. 1(b) shows the change of spectra when varying the grating depth with a step of 2% (5 nm). There are two major points illustrated in Fig. 1: (i) very small changes in topography produce visibly evident and easily experimentally resolvable changes in the ellipsometric spectra; and, (ii) the directions of movement of the SE spectra due to CD and depth variations are nearly orthogonal. The latter point is very important because it means that the CD and depth information can be extracted separately from the SE spectrum.

Figure 2 shows SE simulation results for 75° AOI. Although the change of the spectra with respect to the grating parameter variations can still be easily resolved, the directions of movement of the SE spectra are nearly parallel for CD and depth changes. This graphically indicates that CD and depth are strongly correlated parameters in the off-normal data. Thus, extraction of these quantities from experi-

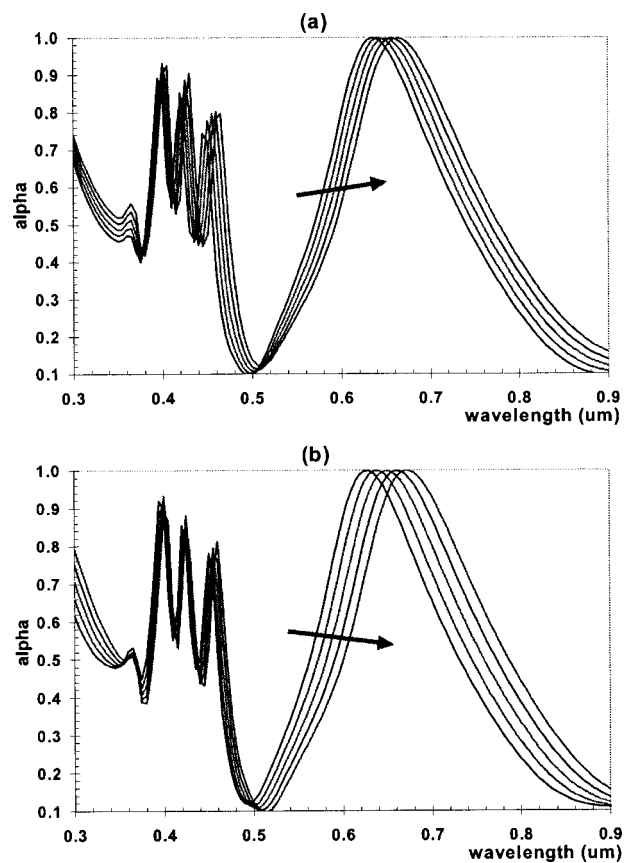


FIG. 2. Off-normal (75°) incidence SE simulation of the submicron MOSFET structure: (a) varying the CD with a step of 2% (1 nm) and (b) varying the gate height with a step of 2% (5 nm).

mental data (containing systematic errors and noise) would be sensitive to significant correlated error effects (relatively large uncertainties in the derived parameters). To re-emphasize one of our major points, the nearly orthogonal movement illustrated in Fig. 1 for the near-normal measurement prevents this parameter correlation problem, and thus allows greater statistical confidence that an accurate approximate solution has been found for the CD and depth.

We have also conducted an experimental demonstration of topography extraction using near-NI SE. The samples were a set of surface relief gratings etched in (100)-orientation single-crystal Si wafers with a SiO_2 layer on the surface. The pattern had nominally 350 nm line/space width, and the SiO_2 was 31.7 nm thick. The samples were then etched using a Lam 9400SE TCP plasma etch system. Seven wafers were etched to different depths (approximately 100–700 nm in 100 nm increments) by changing the etching time. The photoresist mask was stripped before measurements. The time-evolved etched wafers were used to simulate *in situ* data from the etching process. SE measurements were performed using a Sopra GESP-5 rotating polarizer ellipsometer. The samples were accurately aligned so that that grating lines were perpendicular to the optical measurement plane using high-negative-order back-diffracted light. Post-etch cross-section scanning electron microscopy was used to evaluate the line structure profile. The line shapes of the grating were modeled as trapezoids and the features were extracted from the SE data using RCWA combined with Levenberg–Marquardt regression.

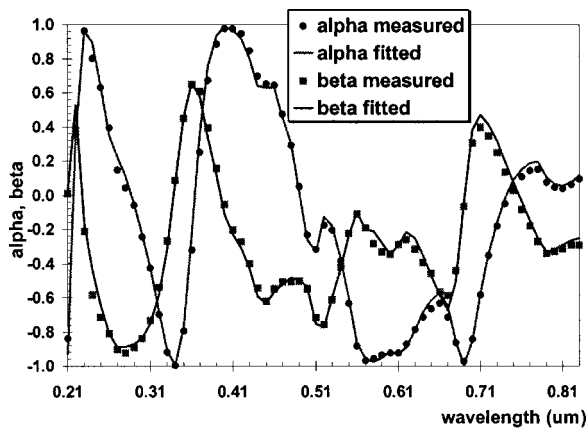


FIG. 3. Near-normal SE experiment and simulation for an etched Si grating.

Figure 3 shows the theoretical and experimental SE spectra at 7° incidence of one sample (~300 nm etch depth) from the surface relief Si gratings. The simulation results fit the SE measured quantities, α and β , very well and capture the sharp features in the measurements. The extracted topography parameters for the sample of Fig. 3 have 95% confidence intervals of 0.4 nm (0.13%) for grating depth, 1.7 nm (0.53%) for the CD, and 0.30° (0.36%) for the sidewall angle. The profile parameters extracted from the nonlinear regression match the SEM measurement within the uncertainty of measurement from the SEM photographs as compared in Table I. In comparison, measurement of this sample at 63.5° and 73° yielded comparable values for all three topographic parameters but increasingly large confidence limits as the AOI increases (see Table I).

The extracted etching depth versus time results from the near-normal measurements are in very good agreement with those measured from SEM, with a root-mean-square error of 9.95 nm for the seven etch times. The actual depth accuracy may be even better, as this comparison is highly sensitive to the position of the two measurements on the wafer and on

TABLE I. Comparison of grating profile extracted from SE and SEM measurements. SE-RCWA values include 95% confidence limits and SEM values include our estimate for errors in manually measuring the photographs.

Parameter	CD (nm)	Depth (nm)	Wall angle	
SEM	323 ± 5	308 ± 5	84.1° ± 1.4°	
SE and RCWA	7°	323 ± 1.7	300 ± 0.4	83.2° ± 0.30°
	63.5°	324 ± 2.8	302 ± 2.7	82.9° ± 0.56°
	73°	321 ± 9.4	302 ± 8.5	82.9° ± 1.8°

our ability to accurately read the SEM photographs (~5 nm uncertainty). These data show the strong potential for *in situ* etching monitoring of grating patterns by using the near-NI SE technique coupled with a vector diffraction theory.

In summary, we have shown that near-NI SE measurements of gratings yield quantitatively accurate CD, depth, and sidewall angle data when applied to periodic patterned structures. The near-NI approach improves the ability to separately extract topography parameters. We have experimentally demonstrated the capability of this technique on 350 nm line/space structures. Our simulations show that there is sufficient sensitivity to measure CDs of 50 nm and below. Use of instrumentation optimized for RDS measurements might further enhance this sensitivity. This technique is easy to implement with existing commercial SE instruments and use of this technique for *in situ* monitoring is possible on many existing vacuum processing systems.

This research is funded in part by the MURI Center for Intelligent Electronics Manufacturing (Contract No. AFOSR F49620-95-1-0524) and the NIST-ATP Program for Intelligent Control of the Semiconductor Patterning Process (Contract No. 70NANB8H4067). The authors would also thank Dr. Weiqian Sun and Dr. Meng-En Lee, for their help on this work.

¹M. Yoshizawa and K. Wada, *International Conference on Microelectronic Test Structures*, Kyoto, Japan, 1990 (IEEE, New York, 1991), p. 135.
²H. P. Kleinknecht and H. Meier, *Appl. Opt.* **19**, 525 (1980).
³S. A. Coulombe, B. K. Minhas, C. J. Raymond, S. S. H. Naqvi, and J. R. McNeil, *J. Vac. Sci. Technol. B* **16**, 80 (1998).
⁴T. Morris, F. L. Terry, Jr., and M. E. Elta, *Proc. SPIE* **1926**, 27 (1993).
⁵R. W. Wood, *Phys. Rev.* **48**, 928 (1935).
⁶B. K. Minhas, S. A. Coulombe, S. S. H. Naqvi, and J. R. McNeil, *Appl. Opt.* **37**, 5112 (1998).
⁷H. Arimoto, S. Nakamura, S. Miyata, and K. Nakagawa, *IEEE Trans. Semicond. Manuf.* **12**, 166 (1999).
⁸M. E. Lee, C. Galarza, W. Kong, W. Sun, and F. L. Terry, Jr., *Proc. Am. Inst. Phys.* **449**, 331 (1998).
⁹X. Niu, N. Jakatdar, J. Bao, C. J. Spanos, and S. Yedur, *Proc. SPIE* **3677**, 159 (1999).
¹⁰B. S. Stutzman, H.-T. Huang, and F. L. Terry, Jr., *J. Vac. Sci. Technol. B* **18**, 2785 (2000).
¹¹R. M. A. Azzam and N. M. Bahara, *Phys. Rev. B* **5**, 4721 (1972).
¹²R. M. A. Azzam and N. M. Bahara, *Ellipsometry and Polarized Light* (North-Holland, Amsterdam, 1987).
¹³M. G. Moharam, E. B. Grann, D. A. Pommet, and T. K. Gaylord, *J. Opt. Soc. Am. A* **12**, 1068 (1995).
¹⁴M. G. Moharam, D. A. Pommet, E. B. Grann, and T. K. Gaylord, *J. Opt. Soc. Am. A* **12**, 1077 (1995).
¹⁵D. E. Aspnes, *J. Vac. Sci. Technol. B* **3**, 1498 (1985).
¹⁶D. E. Aspnes, *IEEE J. Quantum Electron.* **QE-25**, 1056 (1989).